

IGNITION OF PROPELLANT CHARGE BY IGNITER

Dejan Mickovic¹ and Slobodan Jaramaz¹

¹Faculty of Mechanical Engineering, Kraljice Marije 16, 11120 Belgrade, Serbia

The paper includes theoretical and experimental investigations of ignition of propellant charge by igniter. The theoretical studies comprise modelling of two-phase flow of black powder grains and their combustion products in the igniter. Also, the interaction of igniter efflux with the two-phase flow in propellant chamber with granular propellant charge is considered. The experimental investigations of igniter function in open air and in live propellant charge placed in fiberglass propellant chambers are performed. Influence of igniter characteristics on the ignition of propellant charge is established. Verification of the developed theoretical model by the comparison with experimental data is carried out. The presented theoretical-experimental access enables the choice of optimum igniter for ignition of propellant charge

1. INTRODUCTION

Ignition and flamespreading through propellant charges are the vital steps in the whole interior ballistic cycle[1,2]. In this paper we consider the ignition of propellant charge by igniter. An igniter is an element of ignition system of granular propellant charge (Figure 1). The igniter is usually filled with a black powder and its task is to give propellant charge defined energetic impulse in time and space, which should provide uniform ignition of propellant charge. This task realisation depends on mass and type of ignition material in igniter, igniter dimensions, and number, locations and diameter of side holes. The aim of this paper is to enable optimisation of igniter design through theoretical modelling and experimental investigations.

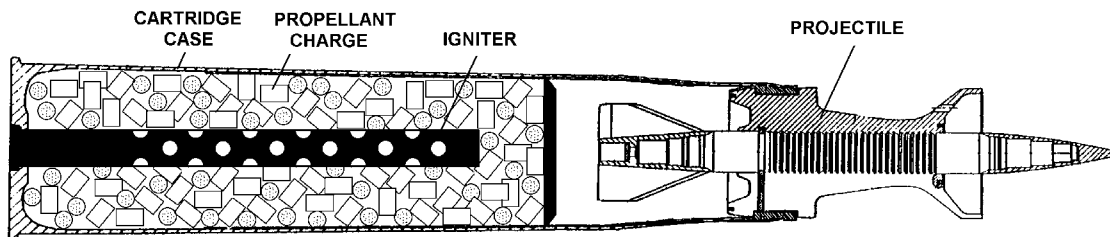


Figure 1. Granular propellant charge with igniter

2. THEORETICAL MODELING

The theoretical modeling of processes in an igniter, interaction of its efflux products with propellant charge and flamespreading through the propellant charge is based on modeling of nonsteady reactive two-phase flow of unburned powder (propellant) grains and their gaseous combustion products. Using certain assumptions and averaging procedures [3], we get the following basic equations of the theoretical model.

Gas-phase mass-conservation equation

$$\frac{\partial(\overline{\varepsilon\rho_g})}{\partial t} + \nabla(\overline{\varepsilon\rho_g \vec{V}_g}) = \frac{\overline{\dot{m}}}{W_{CV}} + \frac{\overline{\dot{m}_{g,fi}}}{W_{CV}} \quad (1)$$

Particle-phase mass-conservation equation

$$\frac{\partial R_p}{\partial t} + \nabla(R_p \vec{V}_p) = -\frac{1}{\rho_p} \cdot \frac{\overline{\dot{m}}}{W_{CV}} \quad (2)$$

where ε , R_p are gas and particles volumetric fraction, ρ_g , ρ_p - gas and propellant density, \vec{V}_g , \vec{V}_p - velocity of gas and solid, $\overline{\dot{m}}$ - rate of interphase mass transfer, $\overline{\dot{m}_{g,fi}}$ - mass flow rate of gases through igniter side holes and W_{CV} is control volume. Single overbar denotes time average; double overbar denotes time average normalised by ε .

Gas-phase momentum-conservation equation

$$\frac{\partial(\overline{\varepsilon\rho_g \vec{V}_g})}{\partial t} + \nabla(\overline{\varepsilon\rho_g \vec{V}_g \vec{V}_g}) = -\varepsilon \nabla \overline{p} - R_p \frac{S_p}{W_p} \langle \vec{F} \rangle^i + \frac{\overline{\dot{m}}}{W_{CV}} \vec{V}_p + \frac{\overline{\dot{m}_{g,fi}}}{W_{CV}} \vec{V}_g \quad (3)$$

Particle-phase momentum-conservation equation

$$\frac{\partial(R_p \rho_p \vec{V}_p)}{\partial t} + \nabla(R_p \rho_p \vec{V}_p \vec{V}_p) = -R_p \nabla \overline{p} - R_p \nabla P_p + R_p \frac{S_p}{W_p} \langle \vec{F} \rangle^i - \frac{\overline{\dot{m}}}{W_{CV}} \vec{V}_p \quad (4)$$

where p is pressure, P_p is intergranular stress and \vec{F} is interphase friction force. Interphase surface average is denoted by $\langle \rangle^i$.

Gas-phase energy-conservation equation

$$\frac{\partial[\varepsilon(\overline{\rho_g \overline{H}_g - \overline{p}})]}{\partial t} + \nabla(\overline{\varepsilon\rho_g \vec{V}_g \overline{H}_g}) = -R_p \frac{S_p}{W_p} \langle q \rangle^i + \vec{V}_p R_p \frac{S_p}{W_p} \langle \vec{F} \rangle^i + \frac{\overline{\dot{m}}}{W_{CV}} \left(\overline{H}_p + h_{c,p} + \frac{\vec{V}_p \vec{V}_p}{2} \right) + \frac{\overline{\dot{m}_{g,fi}}}{W_{CV}} \overline{H}_{g,fi} \quad (5)$$

Particle-phase energy-conservation equation

$$\frac{\partial \left[R_p (\rho_p \bar{H}_p - \bar{p} - P_p) \right]}{\partial t} + \nabla \cdot (R_p \rho_p \bar{V}_p \bar{H}_p) = R_p \frac{S_p}{W_p} \langle q \rangle^i - \bar{V}_g R_p \frac{S_p}{W_p} \langle \bar{F} \rangle^i - \frac{\bar{m}}{W_{CV}} \left(\bar{H}_p + h_{c,p} + \frac{\bar{V}_p \bar{V}_p}{2} \right) \tag{6}$$

where \bar{H}_g, \bar{H}_p are gas and particle total enthalpy, $\bar{H}_{g,fi}$ is total enthalpy of gases coming from the igniter side holes, $h_{c,p}$ is heat of combustion of propellant and q is interphase heat transfer.

The appropriate constitutive laws for determinations of some terms in previous equations are given in [4]. The mass flow rate of black powder gaseous combustion products through igniter side holes is defined from the complete two-phase flow model of igniter real function in the propellant charge. The igniter efflux is governed by the ratio of the pressure in the propellant charge and the corresponding pressure in the igniter (Table 1).

Table 1 Calculation of mass flow rate of gases through igniter side holes

$\frac{\bar{p}}{\bar{p}_{ig}} \leq \left(\frac{2}{\kappa_{BP} + 1} \right)^{\frac{\kappa_{BP}}{\kappa_{BP} - 1}}$	$\bar{m}_{g,fi} = C_D (1 - R_{BP}) A_{fi} \sqrt{\bar{p}_{ig} \rho_{g,BP}} \frac{M_{fi}}{1 + \kappa_{BP} M_{fi}^2} \sqrt{1 + \left(\frac{\kappa_{BP} - 1}{2} \right) M_{fi}^2}$
$\frac{\bar{p}}{\bar{p}_{ig}} > \left(\frac{2}{\kappa_{BP} + 1} \right)^{\frac{\kappa_{BP}}{\kappa_{BP} - 1}}$	$\bar{m}_{g,fi} = C_D (1 - R_{BP}) A_{fi} \sqrt{\frac{2\kappa_{BP}}{\kappa_{BP} - 1} \bar{p}_{ig} \rho_{g,BP}} \left[\left(\frac{\bar{p}}{\bar{p}_{ig}} \right)^{\frac{2}{\kappa_{BP}}} - \left(\frac{\bar{p}}{\bar{p}_{ig}} \right)^{\frac{\kappa_{BP} + 1}{\kappa_{BP}}} \right]$

Remarks: A_{fi} - igniter side holes surface; κ - specific heat ratio of gas; subscript BP denotes black powder

Discharge coefficient C_D and the hole Mach number M_{fi} are determined in accordance with Sneek considerations of the flow in the gun tube side holes. The mass flow rate of unburned black powder through the igniter side holes is calculated by the expression:

$$\bar{m}_{BP,fi} = \frac{C_D}{0.68} R_{BP} A_{fi} \frac{3}{2d_{BP}} (\bar{p}_{ig} - \bar{p}) dt \tag{7}$$

where d_{BP} is the mean equivalent diameter of black powder grain.

Based on the given theoretical model two computer codes are developed:

- IGNITER - for calculation of two-phase flow in the igniter placed in open air,
- TPII - for calculation of interaction of two-phase flows in the igniter and the propellant chamber during ignition phase.

3. EXPERIMENTAL INVESTIGATIONS AND MODEL VERIFICATION

For experimental investigations the special device is used (Figure 2). The basic component of device is the fiberglass tube (the propellant chamber imitation). The tube is transparent and enables flamespreading tracking using the high-speed cinematography. On the tube holes are drilled for acceptance of piezo-gauges for measuring pressures along it. The tube dimensions are given in Figure 3.

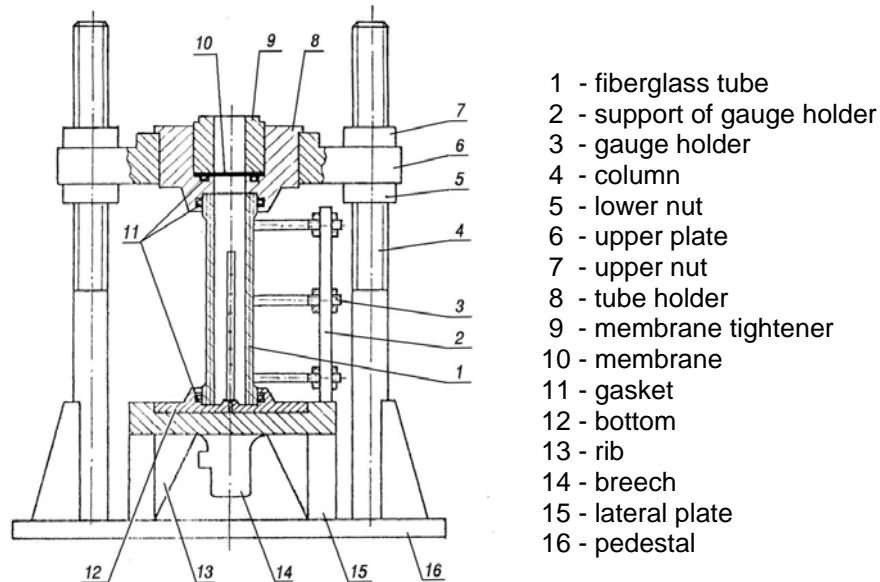


Figure 2. Device for experimental investigation of propellant charge ignition

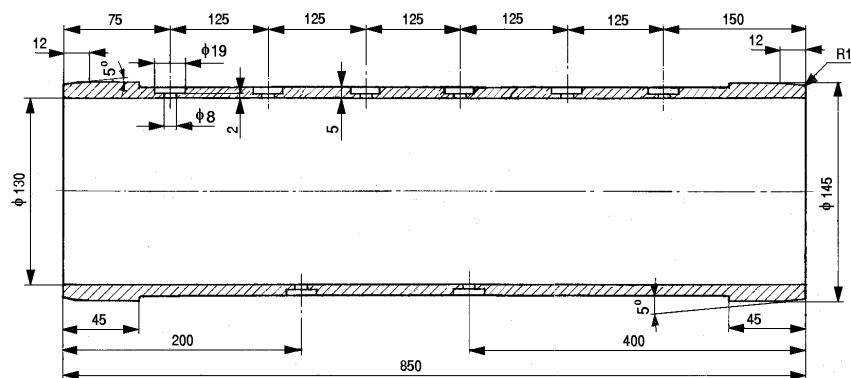


Figure 3. Fiberglass tube

The influence of the igniter on the ignition phase of interior ballistic cycle is studied using four types of igniters. The characteristic dimensions of igniter are shown in figure 4. In Table 2 the basic characteristics of four igniter types are given.

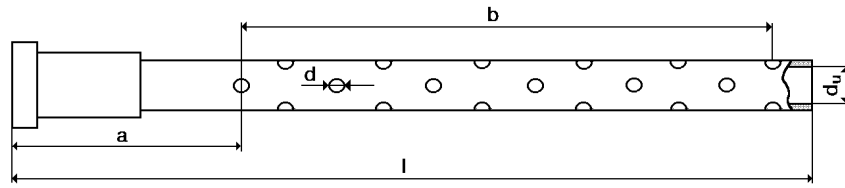


Figure 4. Igniter dimensions (l - igniter length, a - distance from the igniter bottom to the beginning of ignition zone, b - ignition zone length, d-side holes diameter, d_i - igniter interior diameter)

Table 2. Basic characteristics of igniters

	Black pow. mass (g)	Total number of side holes	d (mm)	d_u (mm)	l (mm)	a (mm)	b (mm)
Igniter I	38	32	4.5	10.8	502	166	300
Igniter II	65	32	5.5	14.0	502	166	300
Igniter III	85	36	5.5	14.0	604	184	382
Igniter IV	65	48	4.5	14.0	502	166	300

Igniters are filled with the black powder with the mean equivalent grain diameter of 3.414 mm.

The igniter function in open air is similar to the early phase of propellant charge ignition. In the Table 3 are given the average experimental and calculated values of flamespreading velocity in igniter ignition zones during their function in open air.

As the illustration of compatibility of experimental and calculated results with the program IGNITER in Figure 5 are given results for the igniter II function in open air.

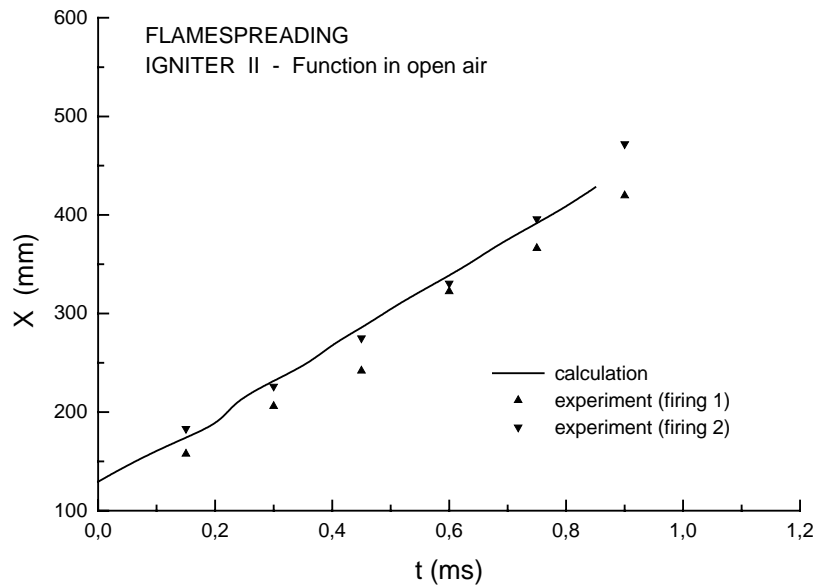


Figure 5. Experimental and calculated results of flame position as a function of time for the igniter II during its function in open air

Table 3. Experimental and calculated average flamespreading velocities in igniter ignition zones during their function in open air

	Igniter I	Igniter II	Igniter III	Igniter IV
$(V_m)_{exp}$	328	357	386	397
$(V_m)_{cal}$	343	356	368	386

The calculations also give the space and time distributions of igniter efflux. In Figure 6 the distributions of total mass of combustion products and unburned grains of black powder till the time of 1.4 ms from the process beginning for the igniter II are given.

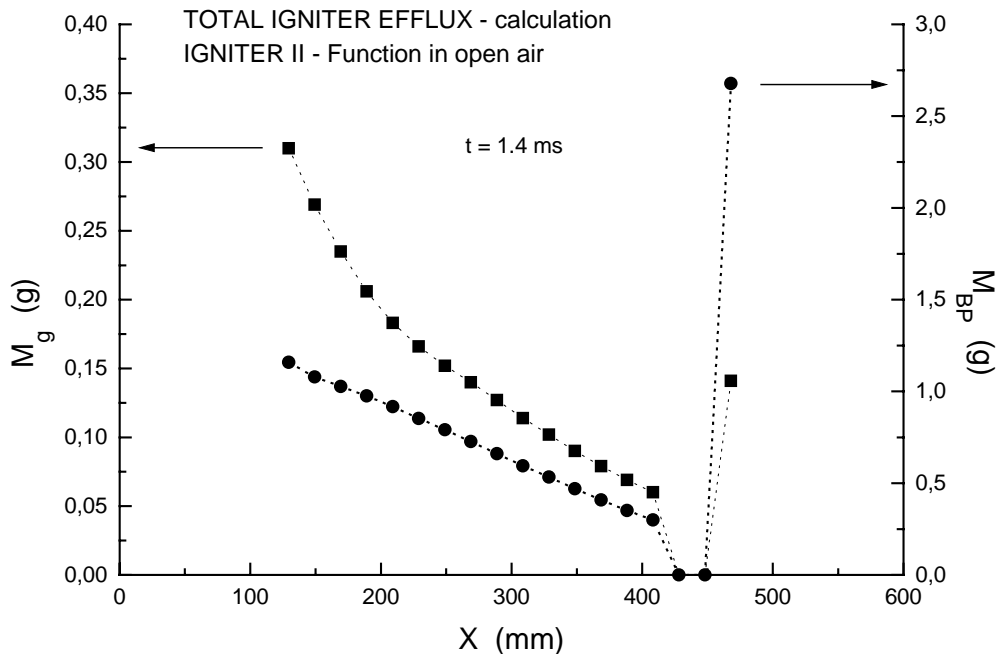


Figure 6. Calculated distributions of total gas and unburned grains masses of black powder expelled from the igniter II during its function in open air

The experiments with live propellant charges give even more realistic picture of igniter function during the whole ignition period of interior ballistic cycle (till reaching the shot start pressure). In Figures 7 and 8 comparisons of calculated and experimental pressures and flamespreading processes for ignition of propellant charge with igniter II are shown. The propellant charge was 6.0 kg of granular 19-tube nitrocellulose propellant.

In Figure 9 comparison of the pressures in the igniter II during its function in open air and live propellant charge are given (for the time $t=1.4\text{ms}$). Also, on that figure the profile of pressure in the propellant charge placed around the igniter is shown

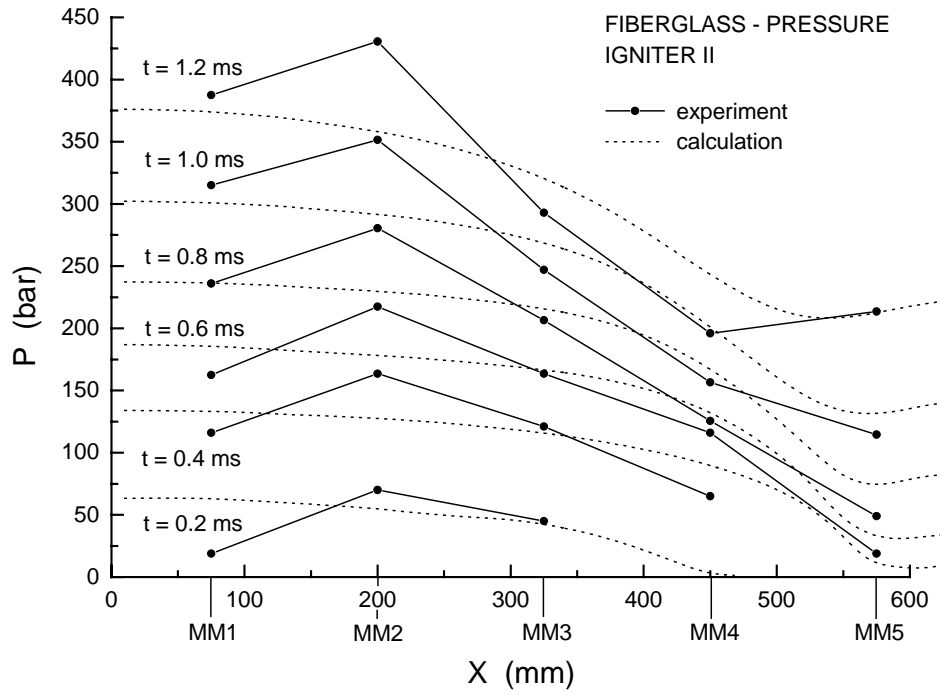


Figure 7. Calculated and experimental distributions of pressures along the propellant chamber during charge ignition by igniter II

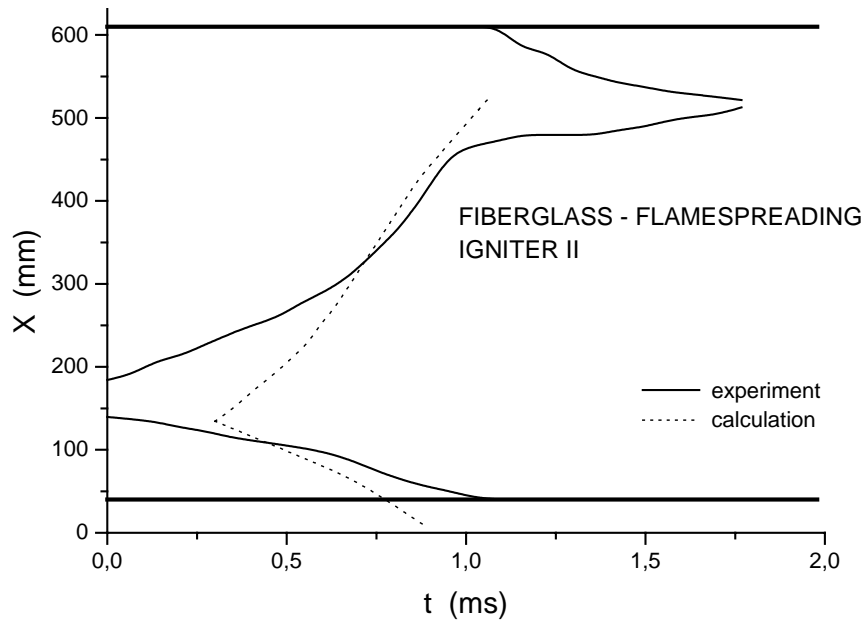


Figure 8. Calculated and experimental flame positions along the propellant chamber during charge ignition by igniter II

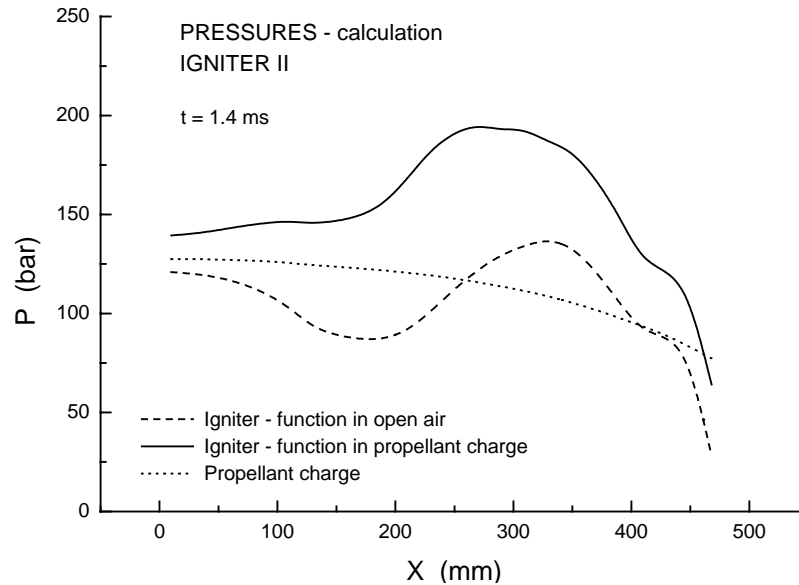


Figure 9. Pressure profiles in the igniter II during its function in open air and live propellant charge

4. CONCLUSIONS

Main conclusions that come from given considerations are:

- The theoretical two-phase models for studying flamespreading through igniter and the propellant charge ignited by igniter are developed,
- Numerical procedures for solving given systems of equations are incorporated in the computer codes IGNITER and TPII,
- Experimental investigations of flamespreading in the igniter in open air and in the live propellant charge ignited by igniter are carried out,
- By comparison of experimental data and computational results verifications of theoretical models are performed.

REFERENCES

1. C.R. Woodley, Modelling Heat Transfer from Conventional and Plasma Igniters to Solid Propellants, *Proceedings of 20th International Symposium of Ballistics, Orlando, 276-282, (2002)*
2. L.M Chang, D.E. Kooker, Ignition and Flame Propagation in Narrow Channels of Solid Propellant: Conventional vs. Plasma Ignition, *Proceedings of 20th International Symposium of Ballistics, Orlando, 283-290, (2002)*
3. S. Jaramaz, D. Mickovic: Modeling Two-Phase Flow of Gas-Solid Particles Mixture during Combustion, *Theoretical and Applied Mechanics, Vol 21., 47-59, (1995)*
4. D. Mickovic, S. Jaramaz: Two-Phase Flow Model of Gun Interior Ballistics, *Proceedings of 19th International Symposium of Ballistics, Interlaken, 65-72, (2001)*